

**ANTIPROLIFERATIVE AND APOPTOSIS
EFFECTS OF *Clinacanthus nutans* LEAF
EXTRACT ON BREAST CANCER CELL (MCF7)**

NOOR ZAFIRAH BINTI ISMAIL

UNIVERSITI SAINS MALAYSIA

2023

**ANTIPROLIFERATIVE AND APOPTOSIS
EFFECTS OF *Clinacanthus nutans* LEAF
EXTRACT ON BREAST CANCER CELL (MCF7)**

by

NOOR ZAFIRAH BINTI ISMAIL

**Thesis submitted in fulfilment of the requirements
for the degree of
Doctor of Philosophy**

February 2023

ACKNOWLEDGEMENT

First and foremost, I am very thankful to Allah S.W.T for blessing me with good health, strength, and the wisdom needed to complete my PhD programme.

I am forever grateful to my supervisor, Associate Professor Dr Hasni Arsad, for his priceless guidance and motivation to complete my thesis. I would like to thank Dr Nur Nadhirah Mohamad Zain for the help and moral support during my studies. They will forever remain my academic mentors. I am equally grateful to my university, Universiti Sains Malaysia, for awarding me the PhD fellowship.

My sincere regards and thanks to all my laboratory mates and science officers from the Advanced Medical and Dental Institute, Universiti Sains Malaysia, for their assistance in my research.

My special thanks go to my beloved parents, Farizah Mahamood and Ismail Hassan, for their continuous support, help, and motivation throughout my studies. Finally, I am grateful to everyone who was involved directly or indirectly in completing my PhD programme.

May Allah bless all of you. Thank you so much.

TABLE OF CONTENTS

ACKNOWLEDGEMENT	ii
TABLE OF CONTENTS	iii
LIST OF TABLES	x
LIST OF FIGURES	xii
LIST OF SYMBOLS	xvi
LIST OF ABBREVIATIONS	xviii
LIST OF APPENDICES	xxi
ABSTRAK	xxii
ABSTRACT	xxiv
CHAPTER 1 INTRODUCTION	1
1.1 Study background.....	1
1.2 Problem statement	3
1.3 Objectives of the study	5
1.4 Scope of the study	6
CHAPTER 2 LITERATURE REVIEW	8
2.1 Human breast.....	8
2.1.1 Normal human breast	8
2.1.2 Cancerous human breast.....	9
2.1.3 Brief epidemiology of breast cancer	11
2.1.4 Breast cancer treatment	12
2.1.4(a) Chemotherapy	12
2.1.4(b) Tissue-targeted therapy.....	12
2.1.4(c) Endocrine therapy	13
2.1.4(d) Radiotherapy	13
2.1.4(e) Surgical interventions	13

2.1.5	Breast cancer cell line: MCF7	14
2.2	Pathophysiology of cancer cells	14
2.3	Programmed cell death mechanism.....	16
2.3.1	Apoptosis signaling pathway	18
2.4	Study of medicinal plants with cancer cells	21
2.5	Medicinal plant: <i>C. nutans</i>	24
2.5.1	Phytochemical compounds of <i>C. nutans</i>	26
2.5.2	Overview of biological activities of <i>C. nutans</i>	27
2.5.2(a)	Anti-viral effect	27
2.5.2(b)	Antimicrobial effect.....	28
2.5.2(c)	Anti-inflammatory effect	28
2.5.2(d)	Antiproliferative and apoptosis effects of <i>C. nutans</i>	28
2.6	<i>In silico</i> molecular study	31
2.6.1	Molecular docking.....	31
2.6.1(a)	Molecular docking of anticancer proteins with natural compounds.....	34
2.6.2	Molecular dynamics simulation	36
CHAPTER 3 METHODOLOGY.....		40
3.1	Introduction	40
3.2	Plant sample	46
3.3	Extraction of <i>C. nutans</i>	46
3.3.1	Maceration of <i>C. nutans</i> leaves	46
3.3.2	Liquid-liquid fractionation	47
3.3.3	Subfractionation of CN-DCM extract	49
3.3.3(a)	Thin layer chromatography (TLC)	50
3.3.3(b)	Column chromatography	51
3.4	Cell culture	54

3.4.1	Complete growth media preparation for MCF7 and MCF 10A cells.....	54
3.4.2	Phosphate-buffered saline (PBS) solution.....	54
3.4.3	Cryoprotectant media	55
3.4.4	Thawing of MCF7 and MCF 10A cells from frozen storage.....	55
3.4.5	Subculturing of the MCF7 and MCF 10A cells	56
3.4.6	Cryopreservation of MCF7 and MCF 10A cells.....	56
3.4.7	Cell counting	56
3.4.8	Cell density.....	57
3.5	Cell viability assay	58
3.5.1	Preparation of stock solution.....	58
3.5.2	Preparation of working solution.....	58
3.5.3	CellTiter 96® AQueous One Solution Cell Proliferation (MTS) assay	59
3.5.4	Selectivity Index (SI)	61
3.6	Cell morphology.....	61
3.6.1	Preparation of acridine orange/propidium iodide (AO/PI) dual-fluorescence dye.....	62
3.6.2	Cell staining.....	62
3.7	Apoptosis analysis.....	63
3.7.1	Preparation of reagent	63
3.7.2	Cell treatment	63
3.7.3	Preparation of MCF7 cells for flow cytometry	64
3.8	Reverse transcription-quantitative polymerase chain reaction (RT-qPCR)...	65
3.8.1	Cell treatment	65
3.8.2	Ribonucleic acid (RNA) extraction.....	65
3.8.3	Complementary DNA (cDNA) synthesis.....	67
3.8.4	Standard curve of cDNA	68

3.8.5	Comparative cycle threshold (CT)	72
3.9	Western blot	73
3.9.1	Cell treatment	73
3.9.2	Preparation of lysis buffer	73
3.9.3	Preparation of total cell lysates	74
3.9.4	Quantification of protein concentration	74
3.9.5	Preparation of reagents for sodium dodecyl sulphate- polyacrylamide gel electrophoresis (SDS-PAGE)	75
3.9.5(a)	Acrylamide/Bis solution (30%)	75
3.9.5(b)	Resolving gel buffer (1.5 M)	75
3.9.5(c)	Stacking gel buffer (1.0 M)	75
3.9.5(d)	Sodium dodecyl sulphate (SDS) (10%)	75
3.9.5(e)	Ammonium persulphate solution (APS) (10%)	75
3.9.5(f)	Tetramethylethylenediamine (TEMED)	76
3.9.5(g)	Resolving gel (12%)	76
3.9.5(h)	Stacking gel (4%)	76
3.9.5(i)	Running buffer (10×)	76
3.9.5(j)	Laemmli sample buffer stock solution (2×)	77
3.9.6	Separation of proteins by electrophoresis	77
3.9.7	Buffers and reagents for Western blot	78
3.9.7(a)	Transfer buffer (10×)	78
3.9.7(b)	Tris-buffered saline (TBS) (10×)	78
3.9.7(c)	TBS-Tween 20 (TBST) (0.1%)	78
3.9.7(d)	Membrane blocking solution (5%)	78
3.9.7(e)	Mild stripping buffer	79
3.9.8	Wet protein transfer	79
3.9.9	Antibody incubation	79
3.9.10	Visualisation of protein bands	80

3.9.11	Polyvinylidene difluoride (PVDF) membrane stripping.....	81
3.10	Phytochemical screening of selected extract.....	81
3.10.1	Gas chromatography-mass spectrometry (GC-MS) analysis.....	81
3.10.2	Drug-likeness and toxicity predictions.....	82
3.11	Molecular docking.....	83
3.11.1	Chemical compounds preparation.....	83
3.11.2	Selection and preparation of protein	83
3.11.3	Preparation of molecular docking analysis	83
3.12	Molecular dynamics simulation	86
3.12.1	Protein-ligand models	86
3.12.2	Initial stage of protein simulation setup.....	86
3.12.3	Energy minimisation	88
3.12.4	Equilibration phases	88
3.12.5	Preparation of molecular dynamics simulation.....	89
3.12.6	Trajectories analysis.....	89
3.12.7	Molecular Mechanics Poisson-Boltzmann Surface Area (MMPBSA).....	90
CHAPTER 4	RESULTS.....	91
4.1	Extraction yields of <i>C. nutans</i> leaves	91
4.2	Antiproliferative effects of crude and fraction extracts.....	91
4.3	Subfraction extracts from CN-DCM extract	94
4.4	Antiproliferative effects of subfraction extracts.....	95
4.5	Cell morphology of MCF7 cells.....	99
4.6	Apoptosis analysis.....	100
4.7	RT-qPCR analysis	103
4.7.1	Purity and concentration of RNA samples.....	103
4.7.2	Standard curve of gene expression.....	104
4.7.3	Comparative CT value	106

4.8	Western blot	107
4.9	Phytochemical screening analysis	109
4.9.1	GC-MS analysis	109
4.9.2	Drug-likeness and toxicity prediction analysis	113
4.10	Molecular docking analysis.....	116
4.11	Molecular dynamics simulation analysis	126
4.11.1	Root-mean-square deviation (RMSD) analysis.....	126
4.11.2	Radius of gyration (Rg) and solvent-accessible surface area (SASA).....	130
4.11.3	Flexibility of the proteins	131
4.11.4	Occupancy of hydrogen bonds.....	137
4.11.5	MMPBSA analysis.....	140
CHAPTER 5 DISCUSSIONS		142
5.1	Extraction yield of the extracts.....	142
5.2	Antiproliferative effect of the <i>C. nutans</i> extracts.....	144
5.3	Cell morphology of MCF7 cells.....	148
5.4	SF2 extract induced apoptosis effect on MCF7 cells.....	148
5.5	Phytochemical screening of SF2 extract	152
5.5.1	Phytochemicals found in SF2 extract.....	152
5.5.2	Drug-likeness and toxicity prediction	154
5.6	Molecular docking.....	155
5.7	Molecular dynamics simulation	157
CHAPTER 6 CONCLUSION.....		161
6.1	Conclusion.....	161
6.2	Limitations of study and future recommendations.....	162

REFERENCES 164

APPENDICES

LIST OF PUBLICATIONS

LIST OF TABLES

	Page
Table 2.1	Medicinal plants in cancer research (<i>in vitro</i>).....22
Table 2.2	List of anticancer proteins and phytochemicals of medicinal plants for computational molecular docking.....34
Table 3.1	List of chemicals and reagents.40
Table 3.2	List of consumables.....41
Table 3.3	List of kits.42
Table 3.4	List of antibodies for Western blot.....42
Table 3.5	List of laboratory equipment.....43
Table 3.6	List of software and hardware for statistical analysis, molecular docking, and molecular dynamics simulation.....44
Table 3.7	The solvents' polarity index and density.48
Table 3.8	Solvent system in column chromatography.51
Table 3.9	Seven experimental conditions for the flow cytometry analysis.65
Table 3.10	The master mix of cDNA synthesis.68
Table 3.11	Ten-fold serial dilution of the cDNA.....69
Table 3.12	The RT-qPCR reaction mixture.69
Table 3.13	Primer sequences used for RT-qPCR assay.....70
Table 3.14	The list of antibodies used in Western blot.....80
Table 3.15	Spacing centred and active binding sites of the targeted proteins.85
Table 3.16	Defaults parameters used in genetic algorithm.86
Table 3.17	Final compositions of the systems in molecular dynamics simulation.....87

Table 4.1	Percentage yield of crude and fraction extracts. The data represents mean \pm SD, n = 3 with different lowercase characters represent significant difference: p < 0.05 using the one-way ANOVA test.	91
Table 4.2	The IC ₅₀ and SI values of crude and fraction extracts. The data represents mean \pm SD, n = 3 with different lowercase characters represent significance difference: p < 0.05 using one-way ANOVA test.	93
Table 4.3	Percentage yield of subfraction extracts from CN-DCM extract. The data represents mean \pm SD, n = 3 with different lowercase characters represent significance difference: p < 0.05 using one-way ANOVA test.	95
Table 4.4	The IC ₅₀ and SI values of subfraction extracts. The data represents mean \pm SD, n = 3 with different lowercase characters represent significance difference: p < 0.05 using one-way ANOVA test.	96
Table 4.5	Range of CT values for the five serial dilutions of cDNA. The data represent mean \pm SD, n = 3.	105
Table 4.6	Compounds obtained from SF2 extract using GC-MS analysis.	111
Table 4.7	Drug-likeness and toxicity prediction of compounds based on Lipinski's rule and OSIRIS Property Explorer. MW: Molecular weight (g/mol); HD: Hydrogen bond donor; HA: Hydrogen bond acceptor; MLOGP: Lipophilicity	114
Table 4.8	Binding energies of the compounds from SF2 extract with targeted apoptotic proteins.	117
Table 4.9	Molecular interactions between targeted apoptotic proteins and the hit phytochemicals.	121
Table 4.10	The Rg and SASA values.	131
Table 4.11	Occupancy of hydrogen bonds throughout the simulations.	138
Table 4.12	Free energy calculations for the simulated systems.	141

LIST OF FIGURES

	Page
Figure 1.1	The simplified flow chart of this present study.....7
Figure 2.1	Cross section of human breast. The diagram was retrieved from Love (2010).9
Figure 2.2	Cross section of cancerous human breast. The diagram was retrieved from Love (2010). 10
Figure 2.3	The seven hallmarks of cancer. 15
Figure 2.4	Diagram of apoptosis and necrosis. The diagram was obtained from Panawala (2017). 16
Figure 2.5	The autophagy process. The diagram was obtained from Mitchell (2012). 18
Figure 2.6	Extrinsic and intrinsic apoptotic signaling pathways. The diagram was obtained from Ichim and Tait (2016). 19
Figure 2.7	The <i>C. nutans</i> plant. (A) <i>C. nutans</i> (B) Leaves (C) Flower. The diagram of the flower was obtained from GlobinMed (2020).25
Figure 2.8	Schematic illustration of molecular docking simulation. The diagram was obtained from Soib (2019).32
Figure 3.1	The detailed flow chart of the present study.45
Figure 3.2	Maceration process of <i>C. nutans</i>47
Figure 3.3	Liquid-liquid fractionation of crude extract using different solvents of different polarities.49
Figure 3.4	Representation of continuous <i>C. nutans</i> leaves extraction.....53
Figure 4.1	Preliminary screening of MCF7 and MCF 10A cells viability treated with crude and fraction extracts at 72 hours. (A) Antiproliferative effect of crude and fraction extracts on MCF7 cells (B) Antiproliferative effect of crude and fraction extracts on MCF 10A cells. The data represents mean \pm SD, n = 3.92

- Figure 4.2 Cell viability of MCF7 and MCF 10A cells treated with subfraction extracts at 72 hours. (A) Antiproliferative effect of subfraction extracts on MCF7 cells (B) Antiproliferative effect of subfraction extracts on MCF 10A. The data represents mean \pm SD, n = 3.....96
- Figure 4.3 Cell viability of MCF7 cells treated with SF2 extract and tamoxifen at 24, 48, and 72 hours. (A) Antiproliferative effect of SF2 extract treated on MCF7 cells at 24, 48, and 72 hours (B) The IC₅₀ values of SF2 extract (C) Antiproliferative effect of tamoxifen treated on MCF7 cells at 24, 48, and 72 hours (D) The IC₅₀ values of tamoxifen. The data represents mean \pm SD, n = 3. The level of significance: p < 0.05 using one-way ANOVA test. Different lowercase characters represent significance differences.....98
- Figure 4.4 The morphological changes of untreated and treated MCF7 cells stained with AO/PI dye at 400 \times magnification using inverted fluorescence microscope. (A) Untreated MCF7 cells (B) SF2-treated MCF7 cells (C) Tamoxifen-treated MCF7 cells. (i) Green fluorescence indicates viable cells (ii) Greenish-yellow with orange fluorescence indicates early apoptotic cells (iii) Red-orange fluorescence indicates late apoptotic cells.99
- Figure 4.5 Apoptosis analysis of MCF7 cells stained with Annexin V-FITC and PI dye (A) Scatter plots analysis of untreated MCF7 cells at 24, 48 and 72 hours (B) Cell percentage of untreated MCF7 cells at 24, 48, and 72 hours (C) Scatter plots analysis of SF2-treated MCF7 cells at 24, 48, and 72 hours (D) Cell percentage of SF2-treated MCF7 cells at 24, 48, and 72 hours (E) Scatter plot analysis of tamoxifen-treated MCF7 cells at 24, 48, and 72 hours (F) Cell percentage of tamoxifen-treated MCF7 cells at 24, 48, and 72 hours. The data represents mean \pm SD, n = 3. The level of significance: p < 0.05 using two-way ANOVA test. Different lowercase characters represent significance differences..... 101
- Figure 4.6 The gene expressions of untreated and treated MCF7 cells at 72 hours. Relative fold changes of genes expressions were expressed

	as mean \pm SD, n=3 for triplicate. The level of significance: $p < 0.05$ using two-way ANOVA test. Asterisk symbol represent significance differences of treated compared to untreated MCF7 cells.	107
Figure 4.7	The protein expression of untreated and treated MCF7 cells at 72 hours. (A) Representative image of proteins expression and β -actin was used as a loading control (B) Relative fold change of protein expressions expressed as mean \pm SD, n=3. The level of significance: $p < 0.05$ using two-way ANOVA test. Asterisk symbol represents significance differences of the treated MCF7 cells compared to untreated MCF7 cells.....	108
Figure 4.8	Two-dimensional structures of β -amyrenol and campesterol. (A) β -amyrenol (B) Campesterol.....	119
Figure 4.9	Compounds interaction with targeted apoptotic proteins. (A) MDM2-P53/ β -amyrenol (B) BCL2/ β -amyrenol (C) MCL1-BAX/ β -amyrenol (D) MCL1-BID/ β -amyrenol (E) caspase-9/ β -amyrenol (F) caspase-8/campesterol (G) caspase-3/campesterol. ...	123
Figure 4.10	RMSD plot of targeted proteins and protein-ligand complexes. (A) MDM2-P53 and MDM2-P53/ β -amyrenol (B) BCL2 and BCL2/ β -amyrenol (C) MCL1-BAX and MCL1-BAX/ β -amyrenol (D) MCL1-BID and MCL1-BID/ β -amyrenol (E) caspase-9 and caspase-9/ β -amyrenol (F) caspase-8 and caspase-8/campesterol (G) caspase-3 and caspase-3/campesterol.....	127
Figure 4.11	RMSF and superimposed visualisation of the unligated and ligated proteins. (A) MDM2-P53 and MDM2-P53/ β -amyrenol (B) BCL2 and BCL2/ β -amyrenol (C) MCL1-BAX and MCL1-BAX/ β -amyrenol (D) MCL1-BID and MCL1-BID/ β -amyrenol (E) caspase-9 and caspase-9/ β -amyrenol (F) caspase-8 and caspase-8/campesterol (G) caspase-3 and caspase-3/campesterol. (i) The RMSF plot (ii) The superimposed visualisation of the unligated and ligated targeted proteins. The labelled numbers indicate the changes in the loop regions.	132

Figure 4.12	The interaction of compounds in the active binding pockets of the targeted proteins at 0 ns (green) and 100 ns (blue). (A) MDM2-P53/ β -amyrenol (B) BCL2/ β -amyrenol (C) MCL1-BAX/ β -amyrenol (D) MCL1-BID/ β -amyrenol (E) caspase-9/ β -amyrenol (F) caspase-8/campesterol (G) caspase-3/campesterol. The labelled residues indicate that the ligands were bound in the binding pockets of the respective proteins.	135
Figure 5.1	The apoptosis pathway of SF2-treated MCF7 cells.	150

LIST OF SYMBOLS

Å	Angstrom
α	Alpha
β	Beta
$\Delta\Delta$	Delta-delta
°C	Degree Celcius
%	Percentage
®	Registered trademark
™	Trademark
$\times g$	Gravitational acceleration
\pm	More or less
=	Equals
\div	Division
\times	Multiplication
+	Plus
<	Less than
>	More than
\geq	Greater than or equal to
~	Approximation
μs	Microseconds
μL	Microliter
μM	Micrometer
μM	Micromolar
A_{260}/A_{280}	Absorbance of 260/Absorbance of 280
cells/mL	Cells/Milliliter
cm	Centimeter

cm ³	Cubic centimetre
CT	Cycle threshold
D	Debye
fs	Femtoseconds
g	Gram
g/mol	Gram/mole
hPa	Hectopascal pressure unit
K	Kelvin
kcal/mol	Kilocalorie/mole
kJ/mol	Kilojoules/mole
kJ/mol/nm	Kilojoules/mole/nanometer
L	Litre
m	Meter
mL	Milliliter
mM	Milimolar
mg/mL	Milligram/mililiter
ng/μL	Nanogram/nanoliter
nm	Nanometer
ns	Nanoseconds
pH	Potential hydrogen
ps	Picoseconds
R ²	Coefficient of determination
rpm	Revolutions per minute
V	Volt

LIST OF ABBREVIATIONS

ADME	Absorption, distribution, metabolism, and excretion
AMBER	Assisted Model Building with Energy Refinement
ANOVA	Analysis of variance
AO	Acridine orange
AO/PI	Acridine orange/propidium iodide
APS	Ammonium persulphate solution
BSA	Bovine serum albumin
Ca ²⁺	Calcium
cDNA	Complementary DNA
CHARMM	Chemistry at Harvard Macromolecular Mechanics
CHL:MEOH	Chloroform:methanol
CN-AQU	Aqueous residue fraction
CN-CHL	Chloroform fraction
CN-CRUDE	Crude methanolic
CN-DCM	Dichloromethane fraction
CN-HEX	<i>n</i> -hexane fraction
CN-MET	Methanol fraction
CO ₂	Carbon dioxide
CT	Cycle threshold
DISC	Death-inducing Signaling Complex
DMEM	Dulbecco's Modified Eagle Medium
DMSO	Dimethyl sulfoxide
DNA	Deoxyribonucleic acid
ECL	Enhanced chemiluminescence
EDTA	Ethylenediaminetetraacetic acid
EGF	Epidermal growth factor
ER	Endoplasmic reticulum
FADD	FAS-associated death domain protein
FBS	Fetal Bovine Serum
GA	Genetic algorithm
GC-MS	Gas chromatography-mass spectrometry

GLOBOCAN	Global Cancer Incidence, Mortality and Prevalence
GROMOS	GRONingen MOlecular Simulation
GROMACS	GRONingen MAchine for Chemical Simulations
H:EA	<i>n</i> -Hexane:ethyl acetate
HER2	Human epidermal growth factor 2
HPLC	High performance liquid chromatography
HSV-2	Herpes simplex virus 2
IC ₅₀	Half-maximal inhibitory concentration
LGA	Lamarckian genetic algorithm
MNCR	Malaysian National Cancer Registry
MLOGP	Moriguchi octanol water partition coefficient
MMPBSA	Molecular mechanics Poisson-Boltzmann Surface Area
MTS	CellTiter 96® AQueous One Solution Cell Proliferation
NADH	Nicotinamide adenine dinucleotide and hydrogen
NADPH	Nicotinamide adenine dinucleotide phosphate
NCI	National Cancer Institute
NCBI	National Center for Biotechnology Information
NIST	National Institute of Standards and Technology
NMR	Nuclear Magnetic Resonance
NO	Nitric oxide
NPT	Isothermal-isobaric ensemble
NTC	Non-template control
NVT	Canonical ensemble
OPLS-AA	Optimized Potentials for Liquid Simulations-All Atom
PBS	Phosphate-buffered saline
PDB	Protein Data Bank
PenStrep	Penicillin-Streptomycin
PES	Phenazine ethosulfate
PI	Propidium iodide
PS	Phosphatidylserine
PTFE	Polytetrafluoroethylene
PVDF	Polyvinylidene difluoride
R _g	Radius of gyration
RIPA	Radioimmunoprecipitation assay

RMSD	Root-mean square deviation
RMSF	Root-mean square fluctuation
RNA	Ribonucleic acid
ROS	Reactive oxygen species
RPMI	Roswell Park Memorial Institute
RSCB	Research Collaboratory for Structural Bioinformatics
RT-qPCR	Reverse transcription-qualitative polymerase chain reaction
SASA	Solvent-accessible surface area
SD	Standard deviation
SDS	Sodium dodecyl sulphate
SDS-PAGE	Sodium dodecyl sulphate-polyacrylamide gel electrophoresis
SF1	Subfraction 1
SF2	Subfraction 2
SF3	Subfraction 3
SF4	Subfraction 4
SF5	Subfraction 5
SF6	Subfraction 6
SF7	Subfraction 7
SF8	Subfraction 8
SF9	Subfraction 9
SI	Selectivity index
SPC	Simple point charge
TEMED	Tetramethylethylenediamine
TLC	Thin layer chromatography
TNF	Tumour necrosis factor
UV	Ultraviolet

LIST OF APPENDICES

- Appendix A Herbarium voucher collection.
- Appendix B Protein BSA standard curve and MCF7 cells protein concentration.
- Appendix C Standard curve of gene expressions.
- Appendix D The phytochemical compounds discovered in the crude and fraction extracts.
- Appendix E GC-MS chromatogram of SF2 extract.
- Appendix F Inhibition constants of compounds with targeted apoptotic proteins.

KESAN ANTIPROLIFERATIF DAN APOPTOSIS EKSTRAK
***Clinacanthus nutans* TERHADAP SEL KANSER PAYUDARA (MCF7)**

ABSTRAK

Clinacanthus nutans ialah tumbuhan herba yang digunakan untuk rawatan alternatif di Asia tropika. Tumbuhan ini mempunyai kesan antiproliferatif terhadap pelbagai barisan sel kanser. Walau bagaimanapun, laluan mekanisme apoptosis dalam sel kanser yang dirawat dengan ekstrak *C. nutans* masih kurang jelas. Oleh itu, objektif kajian ini adalah untuk menentukan kesan antiproliferatif dan apoptosis ekstrak daun *C. nutans* terhadap sel kanser payudara, Michigan Cancer Foundation-7 (MCF7). Untuk mencapai objektif tersebut, daun *C. nutans* telah diekstrak dengan menggunakan 80% metanol, dan selanjutnya difraksinasi dengan pelarut *n*-heksana, diklorometana, kloroform, dan metanol. Ekstrak fraksinasi diklorometana (CN-DCM) menyebabkan kesan antiproliferatif terhadap sel-sel MCF7 pada nilai kepekatan merencat separuh maksimum (IC₅₀) sebanyak $87.33 \pm 1.10 \mu\text{g/mL}$ dengan nilai indeks selektiviti (SI) iaitu 9.07 ± 1.32 . Oleh itu, ekstrak CN-DCM dipilih untuk disubfraksinasi dan ekstrak SF2 menghalang pertumbuhan sel-sel MCF7 dengan nilai IC₅₀ terendah iaitu $23.51 \pm 1.00 \mu\text{g/mL}$ dan mempunyai nilai SI yang tertinggi iaitu 20.46 ± 2.24 . Sel-sel MCF7 yang dirawat dengan ekstrak SF2 mempamerkan tahap apoptosis awal dan akhir, dengan penurunan dalam penanda BCL2 dan peningkatan dalam penanda P53, BAX, BID, caspase-8, caspase-9, dan caspase-3. Sebanyak 32 sebatian yang telah diperolehi daripada analisa kromatografi gas-spektrometri jisim (GC-MS) telah digunakan untuk analisa pengedokan dengan protein apoptosis. Sebatian β -amyrenol mempunyai pertalian pengikatan tertinggi untuk protein apoptosis iaitu MDM2-P53 (-7.26 kcal/mol), BCL2 (-11.14 kcal/mol),

MCL1-BAX (-6.42 kcal/mol), MCL1-BID (-6.91 kcal/mol), dan caspase-9 (-12.54 kcal/mol). Sementara itu, campesterol mempunyai pertalian pengikatan tertinggi untuk protein caspase-8 (-10.11 kcal/mol) dan caspase-3 (-10.14 kcal/mol). Hasil kajian daripada simulasi dinamik molekul mendapati bahawa konformasi protein-ligan adalah stabil dan tidak mempunyai perubahan besar dengan rujukan protein. Semua konformasi protein-ligan mempunyai pertalian pengikatan tinggi untuk simulasi dinamik molekul iaitu MDM2-P53/ β -amyrenol (-23.64 kcal/mol), BCL2/ β -amyrenol (-27.97 kcal/mol), MCL1-BAX/ β -amyrenol (-21.73 kcal/mol), MCL1-BID/ β -amyrenol (-23.75 kcal/mol), caspase-9/ β -amyrenol (-17.39 kcal/mol), caspase-8/campesterol (-15.84 kcal/mol), dan caspase-3/campesterol (-18.67 kcal/mol). Kesimpulannya, kajian ini menunjukkan bahawa ekstrak SF2 mempunyai kesan antiproliferatif terkuat dan mempunyai kesan apoptosis melalui laluan intrinsik dan ekstrinsik dalam sel-sel MCF7. Kajian *in siliko* mendapati bahawa β -amyrenol dan campesterol adalah sebatian penting yang berpotensi dalam memberikan gambaran tentang interaksi molekul dengan protein apoptosis yang disasarkan.

ANTIPROLIFERATIVE AND APOPTOSIS EFFECTS OF *Clinacanthus nutans* LEAF EXTRACT ON BREAST CANCER CELL (MCF7)

ABSTRACT

Clinacanthus nutans is a medicinal plant used for alternative treatments in tropical Asia. This plant has an antiproliferative effect on various cancer cell lines. However, the apoptosis mechanism pathway in cancer cells treated with *C. nutans* extracts remains unclear. Hence, the objective of this study was to determine the antiproliferative and apoptotic effects of *C. nutans* leaf extract on the breast cancer cell line, Michigan Cancer Foundation-7 (MCF7). To address the objective, *C. nutans* leaves were extracted using 80% methanol and further fractionated with the solvents *n*-hexane, dichloromethane, chloroform, and methanol. The dichloromethane fraction (CN-DCM) extract induced an antiproliferative effect on MCF7 cells at a half-maximum inhibitory concentration (IC₅₀) value of 87.33 ± 1.10 µg/mL with a selectivity index (SI) value of 9.07 ± 1.32. Hence, the CN-DCM was selected for subfractionation and SF2 extract inhibited MCF7 cells growth with the lowest IC₅₀ value of 23.51 ± 1.00 µg/mL and had the highest SI value of 20.46 ± 2.24. SF2-treated MCF7 cells exhibited early and late apoptotic phases, with a decrease in the BCL2 marker and an increase in P53, BAX, BID, caspase-8, caspase-9, and caspase-3 markers. A total of 32 compounds obtained in gas chromatography-mass spectrometry (GC-MS) analysis were docked with apoptosis proteins. β-amyrenol compound had the highest binding affinity for apoptosis proteins, namely MDM2-P53 (-7.26 kcal/mol), BCL2 (-11.14 kcal/mol), MCL1-BAX (-6.42 kcal/mol), MCL1-BID (-6.91 kcal/mol), and caspase-9 (-12.54 kcal/mol). Meanwhile, campesterol had the highest binding affinity for caspase-8 (-10.11 kcal/mol) and caspase-3 (-10.14 kcal/mol)

proteins. Molecular dynamics simulation results demonstrated that the protein-ligand conformations were stable and did not alter much compared to the protein references. All protein-ligand conformations had high binding affinity for molecular dynamics simulations, namely MDM2-P53/ β -amyrenol (-23.64 kcal/mol), BCL2/ β -amyrenol (-27.97 kcal/mol), MCL1-BAX/ β -amyrenol (-21.73 kcal/mol), MCL1-BID/ β -amyrenol (-23.75 kcal/mol), caspase-9/ β -amyrenol (-17.39 kcal/mol), caspase-8/campesterol (-15.84 kcal/mol), and caspase-3/campesterol (-18.67 kcal/mol). In conclusion, this study demonstrated that SF2 extract had the strongest antiproliferative effect and induced apoptosis through intrinsic and extrinsic pathways in MCF7 cells. An *in silico* study revealed that β -amyrenol and campesterol are potentially significant compounds that can provide insight into molecular interactions with targeted apoptotic proteins.

CHAPTER 1

INTRODUCTION

1.1 Study background

Cancer is a significant public health concern and the world's most devastating life-threatening disease (El-Saied et al., 2019). It is characterised by dysregulated cell formation, division, and death, as well as uncontrolled cell proliferation (Shaikh et al., 2020). Breast cancer remains a serious public health concern since it has the second highest incidence and mortality rates (Alkabban & Ferguson, 2022). The Global Cancer Incidence, Mortality and Prevalence (GLOBOCAN) reported that breast cancer is responsible for one out of every four female cancer cases and one out of every six female cancer deaths (Sung et al., 2021). The Malaysian National Cancer Registry (MNCR) stated that around 34 out of 100,000 Malaysian women were diagnosed with breast cancer between 2012 and 2016 (Azizah et al., 2019). Although women account for the vast majority of breast cancer patients, a minor proportion of men are also affected (Khan & Tirona, 2021). Chemotherapy continues to be the primary treatment for cancer, despite its significant side effects such as nausea, vomiting, fatigue, and hair loss (Sak, 2012). Additionally, cancer treatment may deteriorate the emotional health of cancer patients due to the high cost of long-term treatment, morbidity, and death (Yabroff et al., 2011). Hence, to address this condition, it is important to determine a non-toxic, economical, conveniently accessible, and highly effective therapeutic drug candidate for cancer treatments (Greenwell & Rahman, 2015; Fu et al., 2018).

The interest in natural products, particularly those derived from medicinal plants, has surged ever since chemotherapeutic treatments are costly, induce morbidity, and have numerous side effects (Siddiqui & Rajkumar, 2012). One of the

beneficial medicinal plants known as *Clinacanthus nutans* has long been recognised for its ethnopharmacological importance for medicinal uses such as diabetes, skin problems (skin rashes and burns), herpes infection, cancer, and inflammation (Sangkitporn et al., 1995; Sakdarat et al., 2009; Shim et al., 2013; Alam et al., 2016). Based on newspaper reports, surveys, and previous research studies, it is indicated that *C. nutans* possesses anticancer effects (Siew et al., 2014) and acts as an antiproliferative agent on a variety of cancer cells, particularly breast cancer cells (Che Sulaiman et al., 2015; Mutazah et al., 2020). One of the breast cancer cell lines is Michigan Cancer Foundation-7 (MCF7), in which this cell line is responsive to the oestrogen receptor. The overexpression of this hormone may increase breast tissue growth, leading to tumour development (Holliday & Speirs, 2011; Lee et al., 2015). MCF7 cells have become a favoured cell line for *in vitro* breast cancer studies because 75% of oestrogen hormone receptors are expressed in breast cancer patients (Krauss & Stickeler, 2020). In previous studies, *C. nutans* leaf extracts have been shown to suppress MCF7 cell proliferation (Che Sulaiman et al., 2015; Fong, 2015; Quah et al., 2017; Wang et al., 2019; Mutazah et al., 2020). However, studies on the efficacy of *C. nutans* fraction solvent extracts with varied degrees of polarity, as well as the evaluation of apoptotic pathway mechanisms on MCF7 cells, are still lacking. Hence, it is essential to find a way to improve existing *C. nutans* research studies to uncover the antiproliferative and apoptotic effects that may be exploited when MCF7 cells are treated with *C. nutans* extract.

1.2 Problem statement

Due to the severe side effects associated with chemotherapeutic treatments, such as nausea, vomiting, fatigue, and hair loss, chemotherapeutic treatments may also have an effect on the patient's pre-existing health and well-being. Hence, alternative treatments are essential to avoid further deterioration of chemotherapy side effects. For this reason, a medicinal plant known as *C. nutans* was selected, as it potentially possessed anticancer effects. In order to enhance earlier research, three publications on antiproliferative effect of MCF7 cells treated with *C. nutans* extracts by Che Sulaiman et al. (2015), Fong (2015), and Quah et al. (2017) need to be improved in terms of a time-dependent experiment. Previous studies revealed that Che Sulaiman et al. (2015) treated MCF7 cells with *C. nutans* extract for 24 hours only, whereas Fong (2015) treated MCF7 cells for 24 hours and 48 hours only. Additionally, Quah et al. (2017) did not mention the incubation time, either 24 hours or 48 hours, for the reported half-maximal inhibitory concentration (IC_{50}) value when MCF7 cells were treated with *C. nutans* methanol leaf extract. As mentioned, this gap can be filled by treating MCF7 cells with selected *C. nutans* extract for 24 hours to 72 hours to demonstrate that cells are indeed going antiproliferation through early apoptosis before progressing to late apoptosis or necrosis. A time-dependent experiment is frequently used to demonstrate that the treated cancer cells are still undergoing antiproliferation owing to apoptotic effects from early to late incubation time (Clarke, 2021).

Despite many studies conducted on MCF7 cells treated with *C. nutans* extract, scant attention has been given to the antiproliferative effect of *C. nutans* extract on normal breast cell line, namely Michigan Cancer Foundation-10A (MCF 10A). Thus, in this study, MCF 10A cells were used to compare the antiproliferative effect of *C.*

nutans extract on MCF7 cells. It is essential to use a normal breast cell line to ensure that *C. nutans* extracts do not promote cytotoxicity in normal breast cells.

Furthermore, it is well-known that cancer cells are sensitive to apoptosis mechanisms, but uncontrolled cancer cell proliferation can lead to apoptosis dysregulation due to overexpression of anti-apoptotic proteins and a lack of expression of pro-apoptotic proteins (Pfeffer & Singh, 2018). Hence, drugs that can impair cancer cells could potentially maintain the regulation of apoptotic mechanisms. In previous research studies, there was an information gap regarding the apoptosis mechanisms of MCF7 cells treated with *C. nutans* extracts. Previous studies by Che Sulaiman et al. (2015), Fong (2015), Quah et al. (2017), Wang et al. (2019), and Mutazah et al. (2020) did not investigate the possible *in vitro* studies of molecular apoptotic pathway mechanisms on MCF7 cells treated with *C. nutans* extract. However, Mutazah et al. (2020) used molecular docking analysis to study the *in silico* molecular interaction of the apoptosis protein known as caspase-3 with *C. nutans* compounds, namely entadamide C and clinamide D. Thus, there is a need for in-depth studies to acquire more information about the apoptosis pathway mechanisms of MCF7 cells treated with *C. nutans* leaf extract.

Previous studies also discovered differences in the *C. nutans* extraction processes for plant phytochemicals. The extraction of medicinal plants is a critical initial step in producing high-quality research output, allowing for more effective screening and purification of natural components in plant extracts (Abubakar & Haque, 2020). Hence, further research into the bioassay-guided approach for the *C. nutans* extraction and the determination of *C. nutans* phytochemical compounds capable of inducing the molecular apoptosis pathway is required.

1.3 Objectives of the study

Main objective:

To determine the antiproliferative and apoptosis effects of selected *C. nutans* extract on MCF7 cells.

Specific objectives:

1. To determine the lowest IC₅₀ value of the selected *C. nutans* extract on MCF7 cells.
2. To determine the cell death phases of MCF7 cells treated with selected *C. nutans* extract by flow cytometry.
3. To determine the apoptosis mechanisms pathway of MCF7 treated with selected *C. nutans* extract using reverse transcription-quantitative polymerase chain reaction (RT-qPCR) and Western blot.
4. To identify the chemical compounds of selected *C. nutans* extract using gas chromatography-mass spectrometry (GC-MS).
5. To study the interaction of the selected compounds with targeted apoptotic protein receptors using molecular docking analysis.
6. To determine the stability and flexibility of the targeted apoptotic protein-ligand interactions using molecular dynamics simulation.

1.4 Scope of the study

In order to address the shortcomings of the problem statement in Section 1.2, this present study focuses on the antiproliferative and apoptosis effects of treated MCF7 cells with selected *C. nutans* extract. Cell viability assay was used to determine the IC₅₀ value of MCF7 cells treated with selected *C. nutans* extract in a dose and time-dependent manner. Then, the treated MCF7 cells viabilities were compared with normal breast cells, MCF 10A. Flow cytometry was used to determine the cell death phases of MCF7 cells treated with a selected extract, and the results were compared to a positive control (tamoxifen) and an untreated control MCF7 cells.

Additionally, the MCF7 cells were observed morphologically to comprehend the evidence of antiproliferation and apoptotic effects of selected *C. nutans* extract. Furthermore, the death mechanisms in MCF7 cells treated with selected *C. nutans* extract through molecular apoptosis pathways were determined using RT-qPCR and Western blot. The presence of phytochemical compounds found in selected *C. nutans* extract was determined using GC-MS analysis. Moreover, molecular docking was used to determine the interaction and binding affinity between targeted apoptotic proteins and the compounds obtained in the GC-MS analysis. The stability and flexibility of the targeted apoptotic protein receptors and the selected compounds conformations were determined using molecular dynamics simulation. Figure 1.1 depicts the brief flow chart of this study.

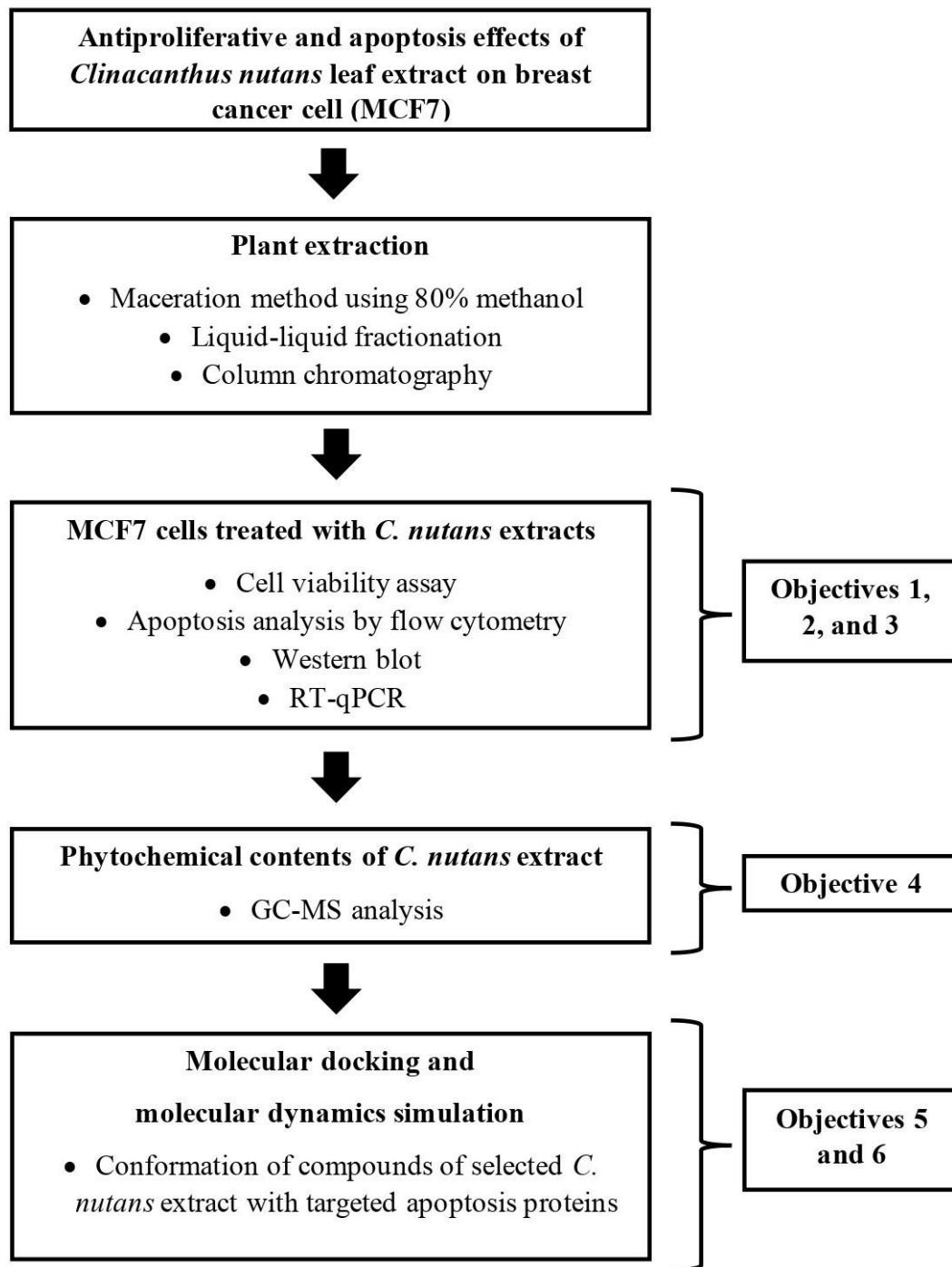


Figure 1.1 The simplified flow chart of this present study.

CHAPTER 2

LITERATURE REVIEW

2.1 Human breast

In both males and females, the breast is characterised as an organ that protrudes from the human body and is located on the upper chest (Dahl et al., 2010). Both males and females have breasts that grow from embryological tissues, although the breasts are not as significant in males as they are in females (Javed & Lteif, 2013).

2.1.1 Normal human breast

Breasts in females are considered extremely important since they have mammary glands, which are the major component of the lactation process that provides milk to feed infants (Javed & Lteif, 2013). Female breast development begins during puberty, when oestrogen and human growth hormone are responsible for breast development and maturation. Subcutaneous fat covers a network of ducts in the breast and nipple tissues during breast development. During pregnancy, the breast responds to the interaction of oestrogens, prolactin, and progesterone in order to prepare for lactation with the help of lobule development called lobuloalveolar maturation. The lobules are small divisions of the breast lobes that are grouped like flower petals and produce breast milk (Hassiotou & Geddes, 2013). The milk runs through a network of small ducts that connect to the larger ducts before exiting the body through the skin's nipple. The nipples were surrounded by the areola, which was supported by the breast connective tissue and ligaments. The human breast also includes a network of nerves, as well as numerous blood vessels, lymph nodes, and lymph vessels (Gupta & Goyal, 2022). Figure 2.1 shows a diagram of the normal human breast.

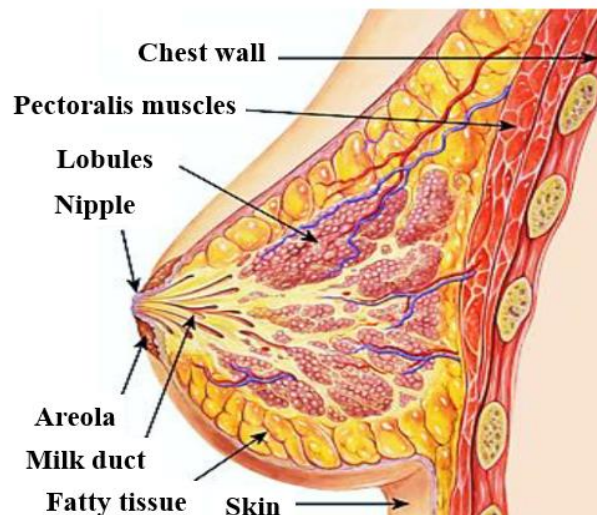


Figure 2.1 Cross section of human breast. The diagram was retrieved from Love (2010).

2.1.2 Cancerous human breast

Breast cancer happens when uncontrolled growth from breast tissue cells in the inner lining or lobules of the milk ducts (Rojas & Stuckey, 2016). Figure 2.2 depicts a diagram of the cancerous human breast. There are two types of breast cancer, namely ductal carcinoma *in situ* (DCIS) and invasive ductal carcinoma (IDC). DCIS is a non-invasive breast cancer that is distinguished by the proliferation of abnormal epithelial cells inside the basement membrane. IDC occurs when abnormal cells form in the lining of the milk ducts and infiltrate breast tissue beyond the duct walls (Sharma et al., 2010). However, if the abnormal cells left untreated, DCIS can progress to ipsilateral IDC (Goh et al., 2019). Breast cancer is further classified based on its response to hormone receptors in cancer cells, specifically as hormone-responsive or hormone-resistant breast cancer (Rojas & Stuckey, 2016). The oestrogen, progesterone, and epidermal growth factor receptors are present in a hormone-sensitive breast cancer cell. On the other hand, hormone-resistant breast cancer refers to the absence of the three previously mentioned hormone receptors (Subhawa et al., 2020). MCF7 is an example of a hormone-responsive breast cancer cell line, whereas

triple-negative breast cancer, MDA-MB-231 cell line is an example of a hormone-resistant breast cancer cell line (Theodossiou et al., 2019). Hormone-responsive breast cancer can be treated with both hormone-based and non-hormone-based chemotherapy, and the incidence of invasion and aggressiveness is lower than in hormone-resistant breast cancer, which can only be treated with non-hormone-based chemotherapy (Isakoff, 2010).

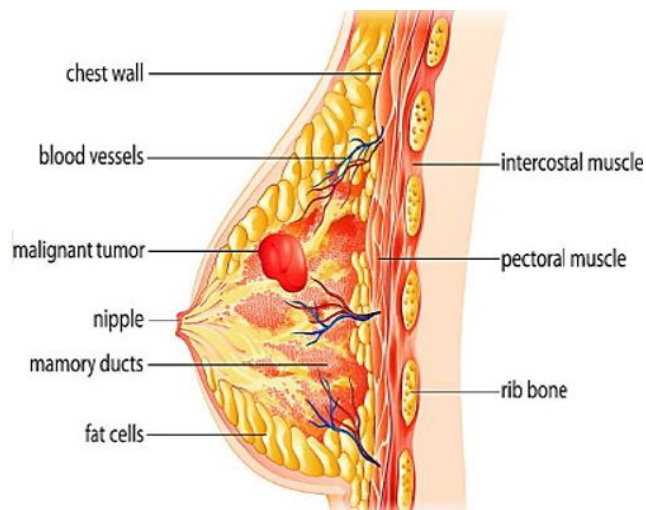


Figure 2.2 Cross section of cancerous human breast. The diagram was retrieved from Love (2010).

The size of the tumour and how it spreads to lymph nodes and other parts of the body determine the stage of breast cancer, which ranges from zero to four. The development of ductal carcinoma occurs at stage zero when the cancer begins in the lobules of the milk duct but does not disseminate to the nearby tissues. Breast cancer in stage one is characterised by a 2 cm in diameter tumour that has not yet spread to the lymph nodes. The 2 cm tumour will spread to nearby lymph nodes during stage two. In stage three, the tumour has grown to a diameter of 5 cm and has begun to spread across the body. Breast cancer progresses to the final stage when it invades distant organs, most notably the brain, bones, lungs, and liver (Sharma et al., 2010).

The symptoms of breast cancer include persistent pain in the breasts and armpits regardless of the woman's monthly cycle, redness on the breast skin, rashes around the nipple, and blood secretion from the nipple. Additionally, the nipple will become inverted or sunken, the breast shape will begin to change, and the breast skin will peel (Amin et al., 2022). Breast cancer risk factors include reproductive and hormonal factors, infertility, obesity after menopause, the use of oral contraceptives, and alcohol intake (Torre et al., 2015). The most successful ways to minimise the risk of breast cancer are increased physical activity, abstinence from alcohol, and a balanced diet to maintain an average body weight (Kushi et al., 2012).

2.1.3 Brief epidemiology of breast cancer

Breast cancer is responsible for 11.7% of all cancer cases, with an estimated 2.3 million new cases each year. It is estimated that one out of every four women will be at risk of developing breast cancer (Sung et al., 2021). In transitioned countries, the incidence rates are 88% greater than in transitioning countries. Northern America, Western Europe, Australia, New Zealand, and Northern Europe have the greatest incidence rates, whereas the Middle East, Eastern Africa, South-Central Asia, and Central America have the lowest incidence rates. Nevertheless, women in transitioning countries have 17% higher mortality rates than those in transitioned countries, with the greatest rates in Western Africa, Melanesia, the Caribbean (Barbados has the highest mortality rate in the world), Micronesia, and Polynesia (Sung et al., 2021).

Breast cancer has been on the rise in most Asian countries, including Malaysia, since 2006 (Medina et al., 2010; Park et al., 2011). The MNCR statistical analysis yielded comparable results, with around 21,634 women newly diagnosed with breast cancer (34 per 100,000 female population) from 2012 to 2016 (Azizah et al., 2019). This study indicated a considerable increase when compared to the MNCR report from

2007 to 2011, with 18,206 new cases diagnosed and 31 per 100,000 women at risk of breast cancer (Azizah et al., 2016). Thus, it is reasonable to assume that the incidence and prevalence of breast cancer have risen steadily over time.

2.1.4 Breast cancer treatment

Treatment for breast cancer may include chemotherapy, tissue-targeted therapy, endocrine therapy, cancer radiotherapy, and surgical interventions referring to different cancer stages.

2.1.4(a) Chemotherapy

Chemotherapy drugs for breast cancer include epirubicin, doxorubicin, paclitaxel, and docetaxel (Maughan et al., 2010). Chemotherapeutic drugs' effectiveness is accompanied by numerous side effects that occur during the treatment. The most common side effects include nausea, hair loss, vomiting, and exhaustion. These side effects were indeed repetitive, tiresome, and resulted in a gradual decline in cancer patients' quality of life (Kool et al., 2015).

2.1.4(b) Tissue-targeted therapy

Human epidermal growth factor 2 (HER2) overexpression in early-stage breast cancer usually needs a tissue-targeted treatment involving the use of trastuzumab, also known as herceptin, in conjunction with additional chemotherapy treatment (Iqbal & Iqbal, 2014). This is because certain types of cancer have a poor prognosis and are particularly resistant to chemotherapy treatment. Trastuzumab is a humanised anti-HER2 monoclonal antibody that works with doxorubicin, epirubicin, or paclitaxel to improve patient survival. The combination of these treatments should be used with caution because a small percentage of patients who have received treatment for more than two years can develop cardiac toxicity (Gajria & Chandarlapaty, 2011).

2.1.4(c) Endocrine therapy

Hormone-responsive breast tumours are treated with endocrine therapy. Tamoxifen, goserelin, exemestane, anastrozole, and letrozole are examples of endocrine therapy. These drugs either block oestrogen or inhibit oestrogen production through the production of hormone agonists, thus preventing oestrogen-sensitive tumours (Maughan et al., 2010).

2.1.4(d) Radiotherapy

High-energy beams are used in radiotherapy to suppress cancer cells in a different way than chemotherapy does. To kill cancer cells in specific areas of the body, external radiation therapy uses a linear accelerator to deliver ionising radiation, such as gamma rays and X-rays (Shirzadfar & Khanahmadi, 2018). Radiation therapy damages deoxyribonucleic acid (DNA) through apoptosis and mitotic cell death. Several early side effects, such as skin dryness, memory loss, oral mucosa, and pneumonitis, will progressively deteriorate if radiation therapy is prolonged (Barazzuol et al., 2020). Thus, medical specialists must approve the therapy session whether the cancer patient is well enough to tolerate radiation therapy.

2.1.4(e) Surgical interventions

If cancer patients have solid tumours, surgical interventions may be used as a primary treatment (Benjamin, 2014). Surgical interventions, in combination with radiotherapy and chemotherapy, can be used to treat solid breast tumours, depending on the stage of the cancer (Chen & Kuo, 2017). Surgical interventions have limitations when it comes to non-solid tumours, such as blood cancers, namely leukaemia and lymphoma. As complications may occur in some post-operation cases, the risk of surgical site infection, post-operative pneumonia, and neutropenia must be closely monitored (Rolston, 2017).

2.1.5 Breast cancer cell line: MCF7

Cancer cell lines are usually employed in cancer research as *in vitro* models to enhance cell understanding of the molecular mechanisms (Mirabelli et al., 2019). In 1973, fifteen years after the discovery of the first breast cancer cell, BT-20 (Lasfargues & Ozzello, 1958), the Michigan Cancer Foundation established and authenticated cancer cells known as MCF7 (Soule et al., 1973). While MCF7 was not the first to be developed, it is still the most frequently used cell line for *in vitro* research. The MCF7 was isolated from the pleural effusion of a 69-year-old white female patient with metastatic adenocarcinoma breast cancer (Lee & Luo, 2022). It is a well-known cell line because of its sensitivity to the hormone oestrogen (Levenson & Jordan, 1997). In the presence of oestrogen, MCF7 cells work fine when introduced into mice or rabbits (xenograft models) for tumorigenic studies, in contrast to other breast cancer cell lines such as MDA-MB-453 and SK-BR-3 (Holliday & Speirs, 2011) that have low metastatic effect. Besides that, *in vitro* MCF7 therapeutic response studies have resulted in promising clinical trials and anticancer drug production, such as faslodex (fulvestrant) (Johnston & Cheung, 2010).

2.2 Pathophysiology of cancer cells

Breast cancer cells have a pathophysiology that is similar to other cancer cells. According to Hanahan and Weinberg (2000), cancer cell pathophysiology is composed of six components that contribute to tumour development. These include self-sufficiency in growth signals, resistance to growth inhibitory signals, evasion of apoptosis, unlimited replication, persistent angiogenesis, and tissue invasion and metastasis. Additionally, cancer-related inflammation is also a part of cancer pathophysiology (Colotta et al., 2009). This pathophysiology of cancer has been named as the hallmarks of cancer (Figure 2.3), and it is being utilised as follow-up

research to better understand the biology of cancer in terms of its potential to develop and spread via metastasis (Hanahan & Weinberg, 2000; Colotta et al., 2009). Each of these components' regulatory mechanisms operates differently, and each advancement may be correlated with the others, resulting in carcinogenesis via many parallel pathways. Anticancer drugs require a schematic method to act as chemopreventive treatments in the human body. The alternative treatment based on the pathophysiology of cancer may inhibit some cancer progression and improve cancer patients' survival indirectly.

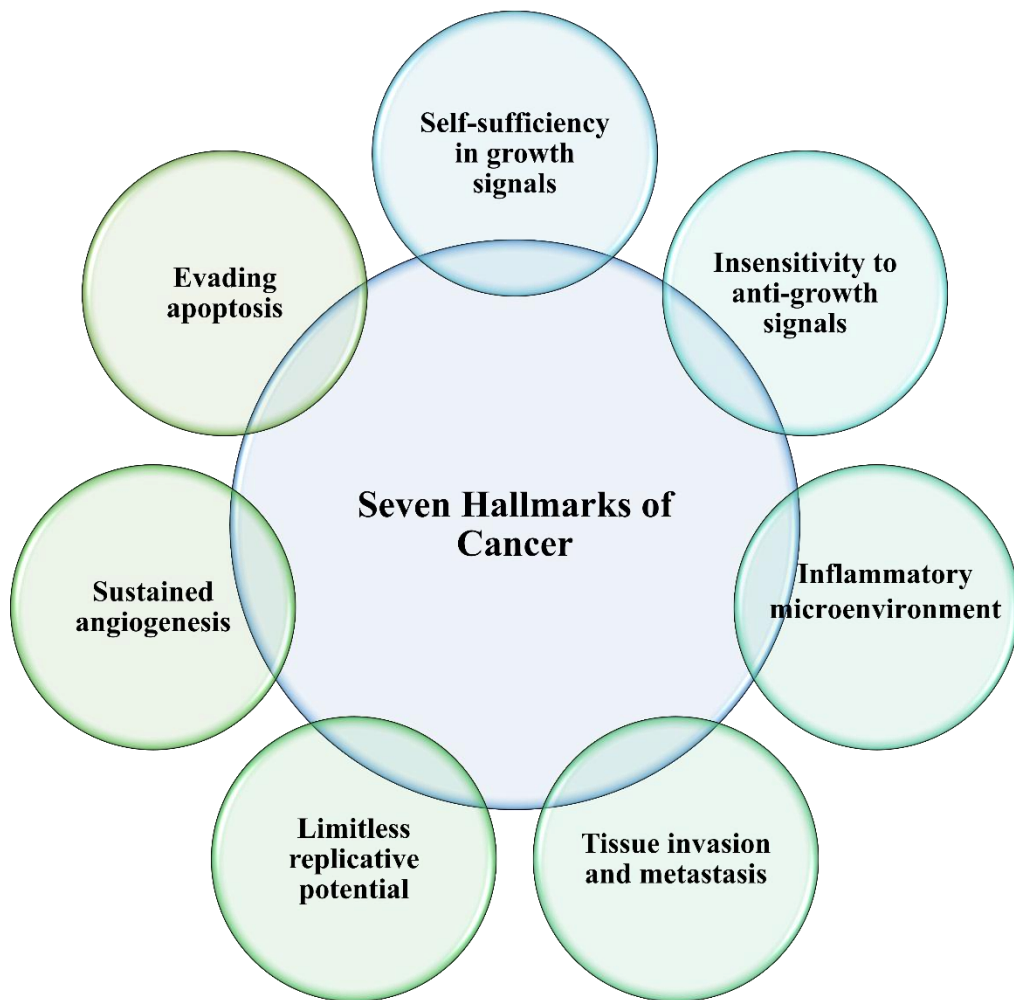


Figure 2.3 The seven hallmarks of cancer.

2.3 Programmed cell death mechanism

The programmed cell death mechanism occurs to regulate and balance cell proliferation by killing damaged cells. Generally, apoptosis, necrosis, and autophagy are the main types of programmed cell death in the body system. Apoptosis is a multi-cellular process where a cell deliberately decides to die. The morphological features of apoptosis programmed cell death, such as nuclear changes (nuclear fragmentation and nuclear chromatin condensation), apoptotic bodies, cell shrinkage, and membrane blebbing (Panawala, 2017), are illustrated in Figure 2.4.

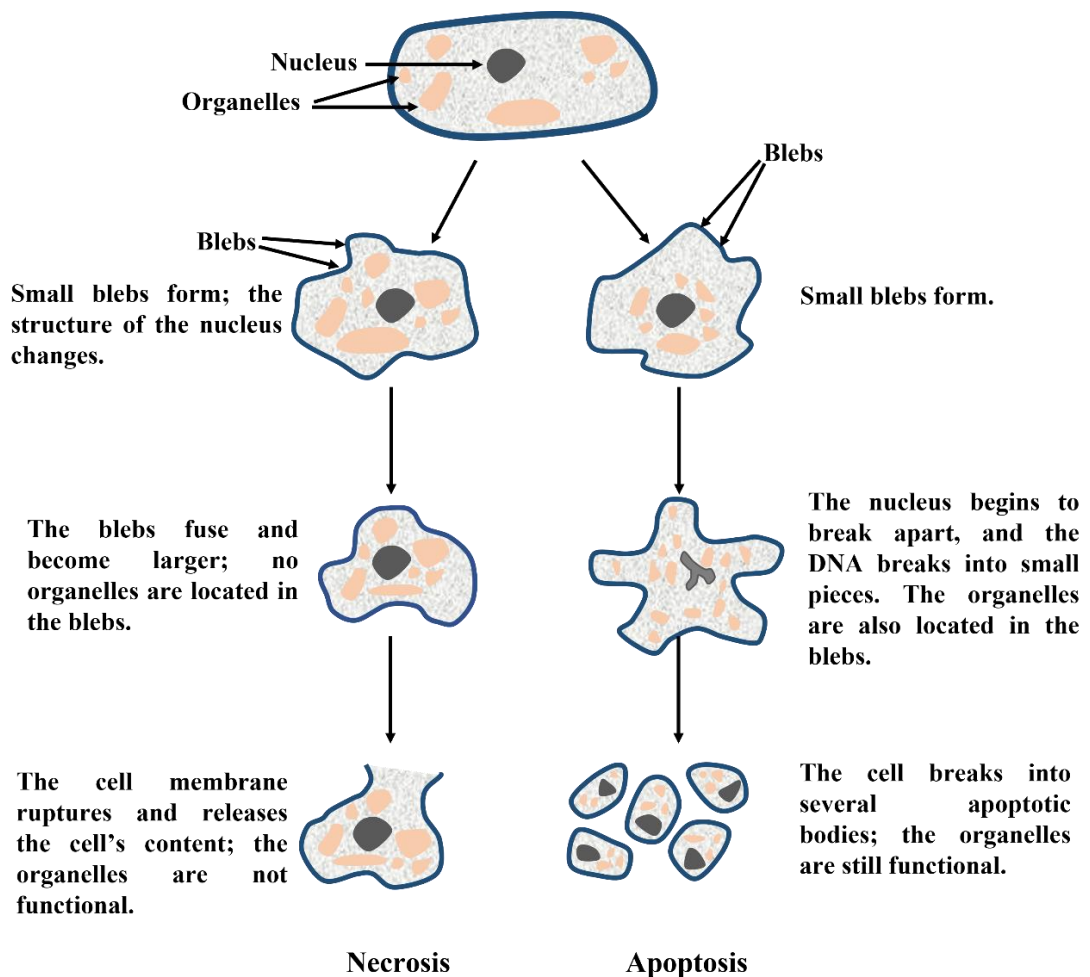


Figure 2.4 Diagram of apoptosis and necrosis. The diagram was obtained from Panawala (2017).

Apoptosis becomes dysfunctional only when the cellular mechanisms that maintain the body in balance induce either too many or too few cell deaths. Many autoimmune disorders, including muscular dystrophy and Alzheimer's, are mainly caused by excessive apoptosis, which causes muscle or nerve cells to die prematurely. Cells that grow uncontrollably indicate that apoptosis is not occurring often enough, which may become cancerous (Kate et al., 2022). Initially, cancer cells are responsive to apoptotic induction, but gradually the cancer cells become resistant due to the dysregulation of apoptotic mechanisms as seen by the overexpression of anti-apoptotic proteins and the absence of pro-apoptotic proteins (Pfeffer & Singh, 2018). In order to maintain cancer cells' apoptotic processes, drug treatments that induce apoptosis mechanisms and weaken the cancer cells are needed.

Necrosis occurs in response to disease or external causes such as toxins, trauma, infection, and physical injury (Vandenabeele et al., 2010; Su et al., 2015). Cellular morphological characteristics of necrosis are cell swelling, organelle dysfunction, cell membrane disruption, and cell lysis (Tonnus et al., 2019). Due to the fact that the apoptosis process is typically normal, necrosis is addressed in an entirely distinct manner from apoptosis. Necrosis is a cell death brought on by external forces, while apoptosis is initiated by the body's natural, healthy processes. As a defensive mechanism during healing, apoptosis is usually normal and helpful to an organism, whereas necrosis is destructive to the same organism. If necrosis is left untreated, it may cause serious harm or death due to gangrene (tissue death due to lack of blood supply or bacterial infection) (Kate et al., 2022). Autophagy has no interaction with phagocytes, where autophagic cell death happens without chromatin condensation but with the presence of cytoplasm (Figure 2.5). During this form of cell death,

cytoplasmic material is trapped within autophagosomes for destruction by lysosomes (Parzych & Klionsky, 2014).

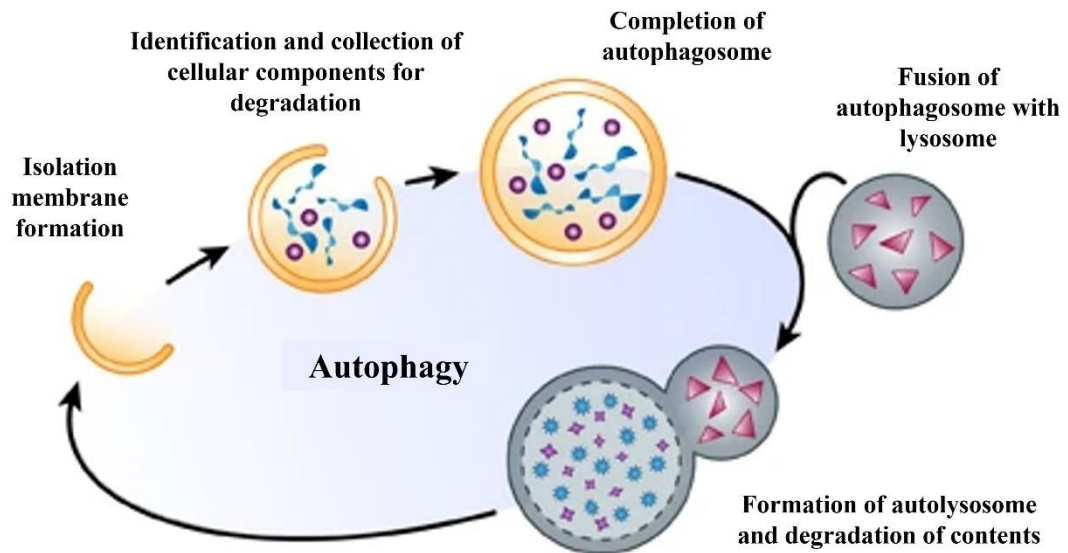


Figure 2.5 The autophagy process. The diagram was obtained from Mitchell (2012).

2.3.1 Apoptosis signaling pathway

Apoptosis signaling pathway has been established as one way of restoring the balance between cell division and death (Adebayo et al., 2017a). Extrinsic and intrinsic pathways are the two main apoptosis signaling pathways (Figure 2.6). An extracellular death signal can be transmitted to the cytoplasm through the extrinsic pathway. The interaction of surface receptors such as death receptors (DR3 to DR6), FAS/CD95, and tumour necrosis factor (TNF) receptor 1 (TNFR1) and TNF receptor 2 (TNFR2) (Klein et al., 2005) with specific ligands activates the extrinsic signal pathway (Degterev et al., 2003). The extrinsic pathway, which can promote receptor trimerisation, is activated when a ligand interacts with death receptors like FAS. To induce trimerisation, FAS-associated death domain protein (FADD) binds to the receptor's intracellular adaptor. For example, TRAIL-R1 and TRAIL-R2 directly attach to

FADD. The adaptor protein is then activated to assist FADD in binding to the procaspase-8 receptor complex (Kumar et al., 2005). Procaspase-8 is essential for molecule-receptor interaction, which activates caspase-8 and then regulates caspase-3 (Kantari & Walczak, 2011). Caspase-8 also cleaves BID into tBID, which moves towards the mitochondria and activates BAK or BAX directly or indirectly (Huang et al., 2016). Hence, BID serves as an interlink between the intrinsic and extrinsic pathways (Kumar et al., 2005).

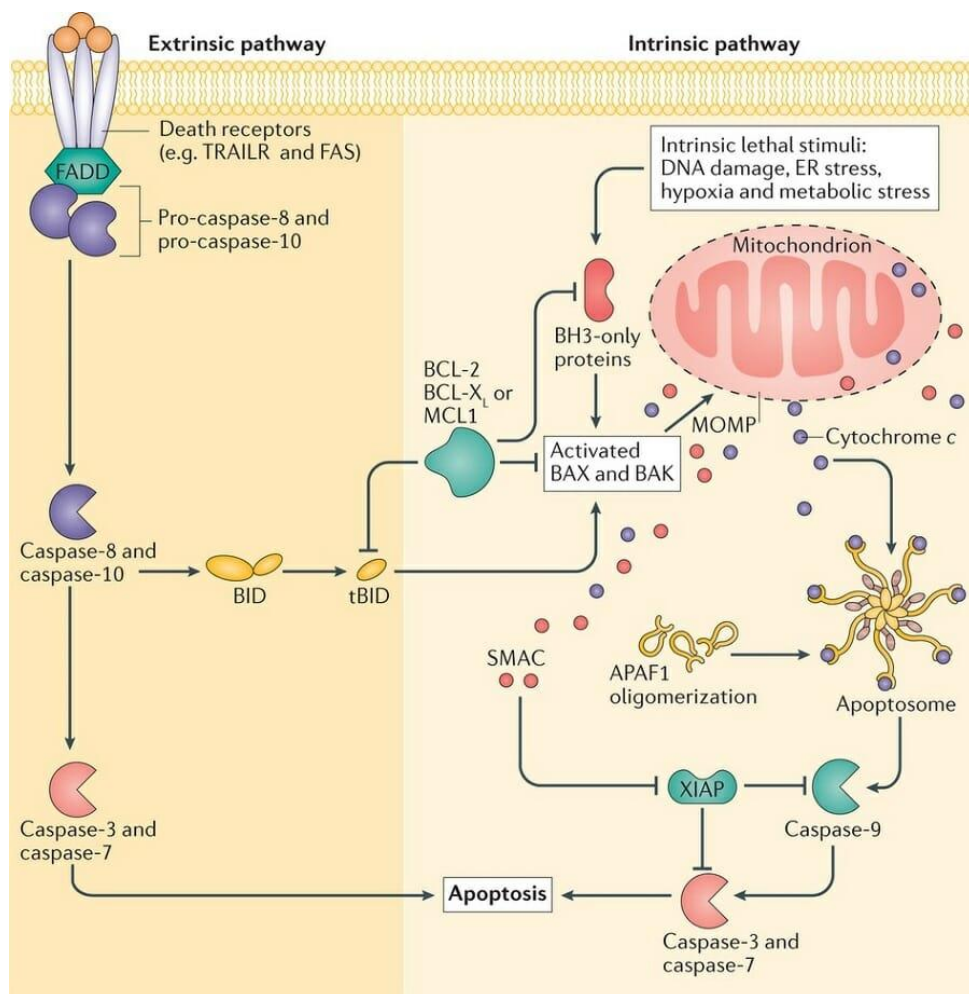


Figure 2.6 Extrinsic and intrinsic apoptotic signaling pathways. The diagram was obtained from Ichim and Tait (2016).

The intrinsic pathway is the activation of mitochondria-mediated apoptosis, which involves the BCL2 protein family. Proteins in the BCL2 family are classified as either anti-apoptotic or pro-apoptotic (Adebayo et al., 2017a). Pro-apoptotic proteins

stimulate cytochrome c release from the mitochondrial intermembrane gap into the cell cytoplasm, whereas anti-apoptotic proteins block this release and thereby prevent apoptotic cell death. The BCL2 family contains both anti-apoptotic proteins (BCL-B, BCL-W, BCL-X, MCL1, and BCL2) as well as pro-apoptotic proteins (BAD, BIM, BID, BAX, BAK, and BOK) that signal mitochondria to release cytochrome c (Gupta et al., 2009). It has been shown that apoptotic proteins can be activated when they are released from their inhibitors, such as MDM2 and MCL1. MDM2 is a domain that acts as a negative regulator of P53. After MDM2 binds to P53, MDM2 decreases the transcriptional activity of the tumour suppressor protein and promotes the inactivation of the tumour suppressor protein (Shi & Gu, 2012). Meanwhile, MCL1 is an anti-apoptotic protein that inhibits the function of proapoptotic proteins such as BAX and BID (Germain et al., 2008; Hockings et al., 2018). Moreover, the anti-apoptotic BCL2 family members are inhibited by the BH3-only protein activator, resulting in activation of BAK, BAX, or BOK, mitochondrial dysfunction, and cytosolic release of apoptogenic proteins like cytochrome c. When mitochondrial integrity is disrupted, the caspase activation cascade is triggered (Leibowitz & Yu, 2010).

Caspase is a cysteine protease family that triggers apoptosis. The execution of apoptotic chromatin degradation will be initiated after caspase is activated (Shi, 2004). There are two types of caspases: apoptotic caspases and inflammatory caspases. Inflammatory caspases known as caspases-1, 4, 5, 11, and 12 have roles in cell death, such as pyroptosis. Meanwhile, apoptotic caspases known as caspases-2, 8, 9, and 10 are categorised as initiator caspases, whereas caspases-3, 6, and 7 are classified as executioner caspases. Initiator caspases will send the apoptosis signal, whereas executioner caspases will carry out the massive proteolysis needed to execute apoptosis (Ke et al., 2016). Caspase malfunction can result in impaired apoptosis and

promote cancer growth. Thus, this mechanism pathway demonstrates the importance of apoptosis in cancer treatment, as any disruption in the apoptosis process can lead to cancer progression.

2.4 Study of medicinal plants with cancer cells

For years, the anti-cancer properties of medicinal plants had been acknowledged. In clinical practise, several anticancer agents of plant origin are employed, including taxol, vincristine, vinblastine, etoposide, irinotecan, and topotecan (Matowa et al., 2020). The National Cancer Institute (NCI) is playing a significant role in the study of medicinal plants usage to cure cancer. Research on ethnomedicine used to treat cancer is still being conducted throughout the world. About 35,000 plant samples from 20 different nations were collected by the NCI, and about 114,000 extracts were evaluated for anticancer activity (Hesari et al., 2021; Manju et al., 2012). Since plant medicine is essential to the discovery and development of new drugs, all these efforts are being made. The demand for medicinal plants increased frequently because they had anticancer activity on cancer cells while having no harmful effects on normal cells. In developing countries, where people traditionally used medicinal plants as their basic form of treatment, several plant species that were examined as herbal medicine were chosen (Ochwang'i et al., 2014). Several medicinal plants that have been employed in *in vitro* cancer treatment were listed in Table 2.1 to substantiate the medicinal claims.

Table 2.1 Medicinal plants in cancer research (*in vitro*).

Medicinal plants	Plant part utilised	Solvent extraction	IC ₅₀ value (µg/mL)	Cell line	Reference	
<i>Physalis minima</i>	Leaves	Hexane fraction	6.00	MCF7	Jaafar (2019)	
		Chloroform fraction	2.00			
		<i>n</i> -butanol fraction	48.00			
		Aqueous fraction	3.00			
<i>Pseudocedrela kotschy</i>	Root and bark	Methanol	87.36	Cervical cancer (HeLa)	Elufioye et al. (2017)	
	Stem and bark	Ethyl acetate fraction	21.53			
<i>Allanblackia gabonensis</i>	Fruit	Crude methanol	39.60	Lung cancer (A549)	Fankam et al. (2017)	
			24.27	MCF7		
			48.06	Pancreatic cancer (PANC-1)		
			20.78	HeLa		
			25.85	A549		
			27.23	MCF7		
			41.28	PANC-1		
			15.43	HeLa		
			25.49	A549		
			Dichloromethane fraction	23.68		MCF7
				31.16		PANC-1
16.38	HeLa					
<i>Moringa oleifera</i>	Leaves	Crude methanol	170.00	MCF7	Mohd Fisall et al. (2021)	
		Hexane fraction	198.00			
		Dichloromethane fraction	5.00			
		Chloroform fraction	6.25			
<i>Christia vespertilionis</i>	Leaves	Crude methanol	94.00	MCF7	Ismail et al. (2021)	
		Hexane fraction	100.00			
		Dichloromethane fraction	24.00			
		Chloroform fraction	74.00			
		<i>n</i> -butanol fraction	190.00			
		Aqueous fraction	114.00			

Table 2.1 Continued.

Medicinal plants	Plant part utilised	Solvent extraction	IC ₅₀ value (µg/mL)	Cell line	Reference	
<i>Allophylus cobbe</i>	Leaves	Hexane	19.46			
		Dichloromethane	6.80			
		Ethyl acetate	19.95			
	Bark	Methanol	11.30			
		Hexane	288.00			
		Dichloromethane	469.30			
<i>Madhuca longiflora</i>	Leaves	Methanol	352.40	Liver cancer (Hep G2)	Thusyanthan et al. (2022)	
		Ethyl acetate	243.80			
	Bark	Hexane	99.49			
		Ethyl acetate	364.80			
	Leaves	Methanol	54.42			
		Hexane	45.86			
Dichloromethane		27.35				
Ethyl acetate		24.56				
<i>Adenanthera bicolor</i>	Bark	Methanol	61.83			
		Hexane	103.70			
	Leaves	Dichloromethane	45.87			
		Ethyl acetate	236.00			
<i>Ficus religiosa</i>	Bark	Ethanol	50.86	Breast cancer (MDA-MB-231)	Saida et al. (2021)	
			4.80	Human neuroblastoma (IMR-32)		
			24.27	Colon cancer HCT 116		
<i>Pongamia pinnata</i>	Seed	Ethyl acetate	84.41	Erythroleukemia (K-562)	Rajput et al. (2021)	
			179.00	HCT 116		
<i>Eclipta alba</i>	Whole plant	Crude methanol	400.00	MCF7	Nelson et al. (2020)	
			470.00	Prostate cancer (PC-3)		
			498.00	Renal cancer (RCC-45)		
			293.27	MCF7		
			238.19			
<i>Tribulus terrestris</i>	Whole plant		218.19	A549	Alshabi et al. (2022)	
			Aqueous			271.07
			Hexane			277.14
			Ethyl acetate			256.38
			Methanol			179.62
			Aqueous			189.70

2.5 Medicinal plant: *C. nutans*

C. nutans (Figure 2.7) also known as Sabah Snake Grass (Zulkipli et al., 2017), is a wonderful plant because of its numerous nutritional and medicinal values (Moses et al., 2015). *C. nutans* other common names are “belalai gajah” or “pokok stawa ular” (Malay), “you dun cao” or “e zui hua” (Chinese), “kitajam” or “daun dandang gendis” (Javanese) and “payayor” or “slaed pang pon” (Thai) (Khoo et al., 2018). *C. nutans* belongs to the kingdom of Plantae, the phylum Magnoliophyta, the class Magnoliopsida, the subclass Asteridae, the order Lamiales, and the family Acanthaceae (Alam et al., 2016). This plant is native to Southeast Asia (Farsi et al., 2016; Zulkipli et al., 2017) and can be found in many countries, such as Malaysia, Thailand, Indonesia, Brunei, and China (Zulkipli et al., 2017; Haida et al., 2020). It grows well in most habitats, consisting of open or dense forest, damp fields, valleys, bushes, mangrove regions, swamps, and marine areas in temperate regions (Meyer & Lavergne, 2004; Alam et al., 2016).

C. nutans is a perennial medicinal plant that has pubescent branches and striate, cylindrical, and glabrescent stems (Alam et al., 2016). It grows to a height of 1 m to 3 m (Zulkipli et al., 2017), with lanceolate or linear-lanceolate leaves that are pubescent when young, then glabrescent as they mature, growing up to 0.3 cm to 2 cm in length and arranged in opposing directions on the curved stem (Fong et al., 2014). The leaves are abaxially elevated and have secondary veins on both sides of the midvein. The flowers are grandular-pubescent and dull red, with a green-based corolla and a calyx. The flowers have dense cymes and branchlets that are covered in five-alpha cymules at the top of the branches and branchlets. The stamen emerges from the neck of the corolla, and the ovary is split into two cells, each with two ovules. The capsule is oval